Food Research International 99 (2017) 790–798

Contents lists available at ScienceDirect

Food Research International

journal homepage: www.elsevier.com/locate/foodres

In vitro digestion of oil-in-water emulsions stabilized by whey protein nanofibrils

Raphaela Araujo Mantovani[a], Ana Cristina Pinheiro[b,c], António Augusto Vicente[b], Rosiane Lopes Cunha[a,*]

[a] Department of Food Engineering, Faculty of Food Engineering, University of Campinas (UNICAMP), 13083-862 Campinas, SP, Brazil
[b] CEB - Centre of Biological Engineering, University of Minho, Campus de Gualtar, 4710-057 Braga, Portugal
[c] Instituto de Biologia Experimental e Tecnológica, Avenida da República, Quinta-do-Marquês, Estação Agronómica Nacional, Apartado 12, 2781-901 Oeiras, Portugal

ARTICLE INFO

Keywords:
Whey protein
Self-assembly
Fibril
Emulsion
In vitro digestion

ABSTRACT

The effect of pH (3 and 7) and varied energy density of a high-pressure homogenization process on the stability of oil-in-water (O/W) emulsions stabilized by whey protein fibrils was evaluated. A dynamic digestion model comprising the simulation of stomach, duodenum, jejunum and ileum, has been used to evaluate O/W emulsions' behavior under gastrointestinal (GI) conditions. The emulsions did not separate phases during the storage period (7 days). The emulsions stabilized by whey protein fibrils were stable under simulated gastric conditions but were destabilized in the simulated intestinal conditions. In a similar way, the whey protein fibrils' dispersion showed a high resistance to proteolytic *in vitro* digestion by pepsin (gastric stage) but was more readily degraded by pancreatin (intestinal stage). This fact confirms the significant impact of the interfacial characteristics on emulsions' digestion. The percentage of free fatty acids (FFA) absorbed in the simulated intestinal conditions (jejunum and ileum) was much lower than the total percentage of FFA released due to the use of WPI fibrils as emulsifier. This work contributes to a better understanding about the behavior of O/W emulsions stabilized by whey protein fibrils within the GI tract; this knowledge is fundamental when considering the final application of this protein in food products.

1. Introduction

Oil-in-water (O/W) emulsions have significant potential for encapsulation of lipophilic bioactive compounds in food products. However, these systems are thermodynamically unstable which can lead to phase separation. Emulsions can be kinetically stabilized with addition of emulsifying agents (McClements, 2005) and by homogenization processes at high pressure, which enable the formation of small droplet sizes (Jafari, Assadpoor, He, & Bhandari, 2008). Whey proteins are widely used as emulsifying/stabilizing agents (Guzey & McClements, 2006; Walstra, 2003) due to their ability to form a thick protective layer onto the interface of oil droplets, increasing emulsion stability (Hu, McClements, & Decker, 2003; Pugnaloni, Dickinson, Ettelaie, Mackie, & Wilde, 2004). Amyloid-like fibrils from whey protein can be used as good gelling agents/thickeners and foam stabilisers because of their high length-to-width ratio (Loveday, Rao, Creamer, & Singh, 2009). Fibrils' potential as a new ingredient in food formulations is due to their robustness and rheological behavior in solution (Loveday, Su, Rao, Anema, & Singh, 2011). Changes in fibril length affect directly functional properties such as foaming, emulsifying or stabilizing capacity (Kroes-Nijboer et al., 2012). The modification of protein fibril length can be promoted by: (i) altering the environmental conditions during or after fibril formation such as temperature *versus* heating time, ionic strength, pH and composition (Blijdenstein, Veerman, & Van der Linden, 2004; Kroes-Nijboer et al., 2012; Loveday et al., 2011; Mantovani, Fattori, Michelon, & Cunha, 2016b; Serfert et al., 2014) or (ii) by applying mechanical treatments after the process of fibril formation using high shear or moderate shear (Oboroceanu, Wang, Magner, & Auty, 2014; Oboroceanu et al., 2011; Peng, Simon, Venema, & Van der Linden, 2016; Serfert et al., 2014). Previous studies have reported that mixing of emulsions stabilized by native whey proteins at low (Blijdenstein et al., 2004) or high fibril concentrations (Peng et al., 2016) can induce a depletion-flocculation process.. However, the potential of fibril systems as a single emulsifier has not been fully investigated.

Understanding physiological events such as the digestion process of fibrils is of great importance for their application in food formulations. *In vitro* digestion of fibrils produced from β-lactoglobulin (Bateman,

* Corresponding author.
E-mail address: rosiane@unicamp.br (R.L. Cunha).

http://dx.doi.org/10.1016/j.foodres.2017.06.049
Received 22 February 2017; Received in revised form 17 June 2017; Accepted 21 June 2017
Available online 22 June 2017

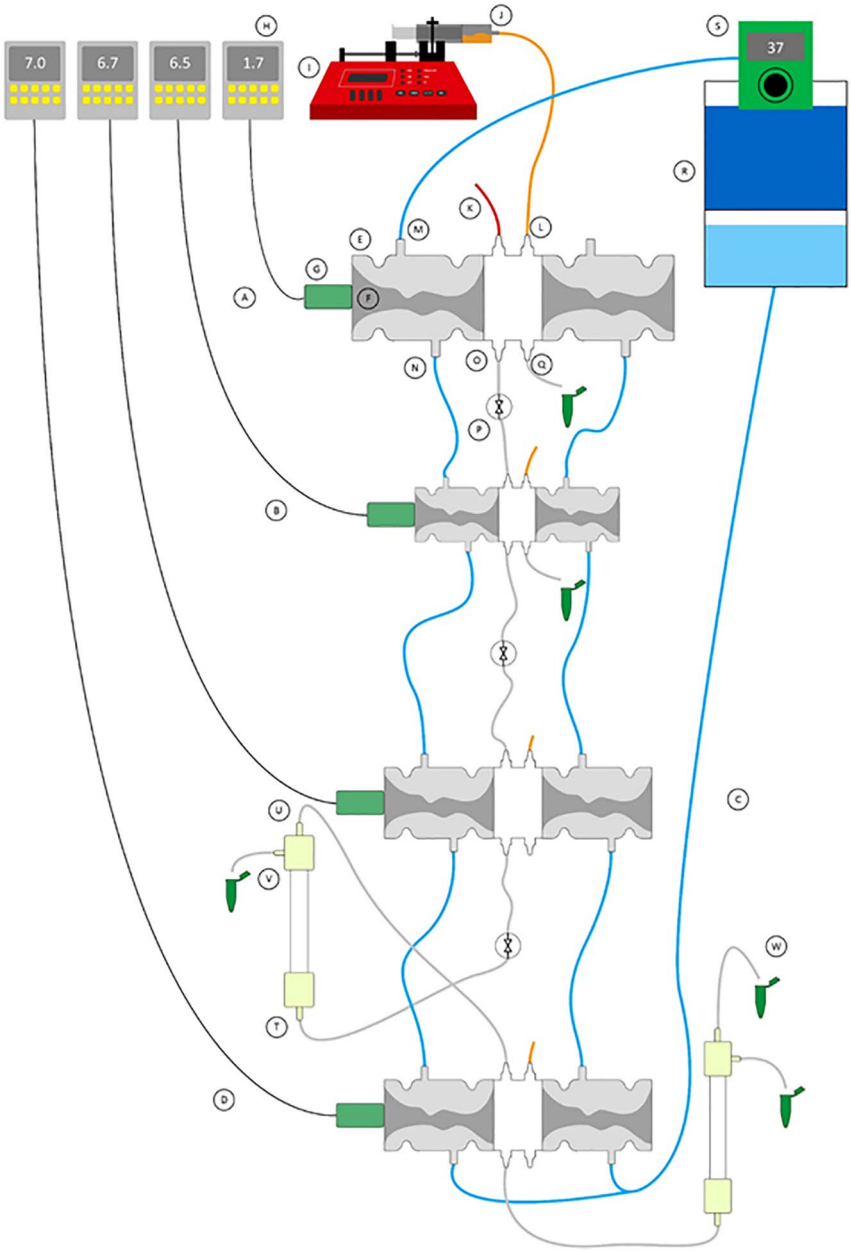

Fig. 1. Representative schematic of the *in vitro* GI system where A) stomach compartment; B) duodenum compartment; C) jejunum compartment; D) ileum compartment; E) glass reactor; F) silicon bags; G) pH electrode; H) pH monitor; I) syringe pump; J) digestion secretion syringe; K) sample inlet; L) digestion secretion inlet; M) water at 37 °C inlet; N) water outlet; O) digestion products outlet; P) valve; Q) digestion sample; R) water bath at 37 °C; S) water heater; T) hollow fiber membrane inlet; U) hollow fiber membrane outlet; V) jejunum/ileum filtrate and W) ileum delivery sample.

Ye, & Singh, 2010) or whey protein isolate (Lassé et al., 2016) has been reported. However, the digestibility of these nanostructures at oil-water interface should be also evaluated if they are applied as emulsifiers since the digestion response of emulsions depends not only on the nature of food matrix but also to their interfacial properties (Pafumi et al., 2002). The bioavailability of lipid components when emulsions are applied as delivery systems is another relevant point that must be taken into consideration. Lipolysis begins in the stomach at low acidic pH (around 2), which is ideal for gastric lipase activity. In this step, mainly free fatty acids and diacylglycerols are produced from the ingested triacylglycerol hydrolysis. The lipid hydrolysis occurring in the stomach facilitates the subsequent lipid hydrolysis in the duodenum by pancreatic lipase since it facilitates fat emulsification and, consequently, lipase activity (Pafumi et al., 2002). Thus, the lipid digestion process consists in an interfacial reaction since its occurrence depends on lipase adsorption onto the oil droplet surface (Torcello-Gomez, Maldonado-Valderrama, Martin-Rodriguez, & McClements, 2011). Considering these aspects, studying the response of the interfacial composition of emulsions subjected to the gastrointestinal tract conditions is important for a better control of lipid bioavailability (McClements, Decker, & Park, 2007; Mun, Decker, & McClements, 2007) and to define the final application of the encapsulation system.

This work aimed at studying the influence of pH (3 and 7) and energy density of the high-pressure homogenization process on the stability of O/W emulsions stabilized by whey protein fibrils. A dynamic digestion model comprising the simulation of stomach, duodenum, jejunum and ileum, has subsequently been used to evaluate the behavior of O/W emulsions under gastrointestinal conditions. Whey protein fibrils dispersed in aqueous solution were also subjected to simulated gastrointestinal conditions to understand the influence of fibrils on emulsions' digestibility.

2. Materials and methods

2.1. Materials

Soybean oil (Soya, Bunge Alimentos S.A., Gaspar, Brazil) was purchased in the local market. Whey protein isolate (WPI) (protein content

of 90.6 ± 0.5% w/w) was obtained from New Zealand Milk Products (ALACEN 895, Wellington, New Zealand). Pepsin from porcine gastric mucosa, lipase and pancreatin (8 × USP) from porcine pancreas, bile extract porcine and other reagents of analytical grade were purchased from Sigma-Aldrich (St. Louis, USA). Acetone was obtained from Fisher Chemical (Loughborough, UK) and sodium hydroxide and phenolphthalein from Panreac (Barcelona, Spain).

2.2. Fibril formation

Fibril formation was performed as described in a previous work (Mantovani et al., 2016b). A WPI stock solution (2% w/w) was prepared at room temperature by dissolving the protein powder in Milli-Q water and using magnetic stirring for 2 h to guarantee the complete dissolution of the protein. The pH of the protein solution was adjusted to 2 with 3 mol·L^{-1} HCl. Subsequently, the WPI stock solution was filtered through 0.45 μm low-protein adsorbing filters (Millex-HV®, Millipore, Billerica, USA) and heat-treated at 80 °C during 20 h under mild stirring. After heating, the system was immediately cooled to room temperature using an ice bath. Afterwards, the fibrillar dispersion pH was adjusted to 3 and 7 using 2 mol·L^{-1} NaOH.

2.3. Emulsion preparation

The aqueous phase of oil-in-water (O/W) emulsions consisted of 2% (w/v) WPI fibril dispersion at pH 3 and 7. O/W emulsions were prepared at 25 °C by homogenizing soybean oil with the aqueous phase using a rotor stator Ultra-Turrax (T 25, Ika-Werke, Staufen, Germany) at 14,000 rpm for 3 min followed by passage through a high-pressure homogenizer (Nano DeBEE, BEE International, South Easton, USA) at 3000 (P_3) or 20,000 (P_{20}) psi (20.7 or 137.9 MPa), for 1 (C_1) or 20 (C_{20}) cycles. For all systems, the oil phase content was fixed at 30% (w/w). The energy density input during high-pressure homogenization of O/W emulsions stabilized by WPI fibrils was calculated as power × time / volume (Karbstein & Schubert, 1995). Emulsions were analysed for creaming stability and particle size distribution.

2.4. In vitro digestion

A dynamic *in vitro* system was used to evaluate the digestibility of two systems at pH 3: (i) 2% w/v WPI nanofibril dispersion and (ii) O/W emulsion stabilized by WPI nanofibrils prepared as previously described in section 2.3. A gastrointestinal model constituted by four compartments (stomach, duodenum, jejunum and ileum) as shown in Fig. 1 that simulated the main events occurring during digestion was used to perform this experiment as previously described by other authors (Pinheiro, Coimbra, & Vicente, 2016). The average physiological conditions of gastrointestinal tract were simulated by the continuous addition of gastric, duodenal, jejunal and ileal secretions at pre-set flow rates of 0.33, 0.66, 2.13 and 2.0 mL·min^{-1}, respectively. The sample (60 mL) was introduced into the dynamic gastrointestinal system (gastric compartment) and, at a predefined time, a constant volume of chyme was transferred to the subsequent compartment. The experiment lasted for a total of 5 h, of which 2, 1, 1 and 1 h were the duration times of gastric, duodenal, jejunal and ileal steps, respectively. The gastric secretion consisted of a gastric electrolyte solution (NaCl 4.8 g·L^{-1}, KCl 2.2 g·L^{-1}, $CaCl_2$ 0.22 g·L^{-1} and $NaHCO_3$ 1.5 g·L^{-1}), pepsin (600 U·mL^{-1}) and lipase (40 U·mL^{-1}). The pH was controlled by secreting 1 mol·L^{-1} HCl to follow a predetermined curve (from 4.8 at t = 0 to 1.7 at t = 120 min) according to Supplementary Material Fig. 1S. The duodenal secretion consisted of the small intestinal electrolyte solution (SIES) (NaCl 5 g·L^{-1}, KCl 0.6 g·L^{-1}, $CaCl_2$ 0.25 g·L^{-1}) added to a mixture of 4% (w/v) porcine bile extract and 7% (w/v) pancreatin solution. The jejunal secretion fluid consisted of SIES containing 10% (v/v) porcine bile extract solution. The ileal secretion fluid consisted of the SIES. In the different compartments simulating the intestinal digestion the pH was controlled by the addition of 1 mol·L^{-1} $NaHCO_3$ solution to set-points of 6.5, 6.8 and 7.2 for simulated duodenum, jejunum and ileum, respectively. The jejunum and ileum compartments were connected with hollow-fiber devices (SpectrumLabs Minikros®, M20S-100-01P, USA) to simulate the adsorption of lipid digestion products. During digestion, samples were collected directly from the lumen of the different compartments, from the jejunal and ileal filtrates and from the ileal delivery. The fibril dispersion was analysed for morphology and an electrophoresis was performed and the emulsion was analysed for size, microstructure and free fatty acids. The samples were tested in the dynamic gastrointestinal model in duplicate.

2.5. Fibril characterization

2.5.1. Zeta potential

The surface electric charge density of the fibril dispersion at pH 3 and 7 was determined before emulsion preparation according to the methodology described by Mantovani et al. (2016b). Samples were diluted to a concentration of about 0.05% (w/v) in Milli-Q water. Immediately before being placed in the measuring chamber of microelectrophoresis (Zetasizer Nano-ZS, Malvern Instruments Ltd., Malvern Hills, UK). The Smoluchowski mathematical model was used to convert the electrophoretic mobility measurement into zeta potential values. Samples were measured in triplicate at 25 °C.

2.5.2. Transmission electron microscopy (TEM)

TEM micrographs were obtained as described by a previous work (Mantovani et al., 2016b). A droplet of the diluted WPI fibril dispersions at different stages of digestion was put onto a carbon support film on a copper grid. The excess of water was removed using a filter paper. Subsequently, a droplet of 2% (w/v) uranyl acetate was put onto the grid and again removed with a filter paper. Electron micrographs were taken using a Libra 120 transmission electron microscope (Carl Zeiss AG, Oberkochen, Germany) operating at 80 kV equipped with an in-column OMEGA energy filter and a Olympus CCD camera 14 bits with 1376 × 1032 resolution for fibril characterization at pH 3 and 7 and a EM 902A transmission electron microscope (Carl Zeiss AG, Oberkochen, Germany) for fibrils at different stages of digestion.

2.5.3. Native polyacrilamide gel electrophoresis (native-PAGE)

WPI fibril dispersions at different stages of digestion were by native-PAGE according to Laemmli (1970), using a gel of 1.5 mm thickness with 10% acrylamide running gel and 5% stacking gel. A Mini-Protean electrophoresis system (Bio-Rad Laboratories, Hercules, USA) was used for the measurements at a constant voltage of 120 V.

WPI fibril dispersions were diluted in ultrapure water (Direct-Q3, Millipore, USA) (2 mg WPI/mL) and mixed at 1:1 ratio with an electrophoresis sample buffer (containing 50 mmol·L^{-1} Tris-HCl, 10% (v/v) glycerol, 0.1% (w/v) bromophenol blue). Then, 15 μg aliquots were loaded onto the polyacrilamide gels. After each run, the gels were immediately stained using 0.25% (w/v) Comassie Brilliant Blue for 2 h and destained with a solution composed of ethanol/glacial acetic acid/water (4.5:1:4.5) for 3 h with five changes.

2.6. Emulsion characterization

2.6.1. Creaming stability

Creaming stability was evaluated according to Mantovani, Cavallieri, and Cunha (2016a). The emulsion (25 mL) was poured into a graduated cylindrical glass tube (internal diameter = 25 mm, height = 95 mm) immediately after preparation. Afterwards, the tube was sealed with a plastic cap and stored at 25 °C. The emulsion phase separation was visually analysed during 7 days.

2.6.2. Particle size distribution (PSD)

The particle size of the emulsions was measured after 2 days of

storage and at different stages of digestion by dynamic light scattering (Zetasizer Nano ZS, Malvern Instruments, Worcestershire, UK). The PSD was presented as volume based size distribution.

Mean droplet size of each peak was reported as average hydrodynamic diameter ($\overline{D}$), which was calculated according to Eq. (1).

$$\overline{D} = \sum x_i D_i \quad (1)$$

where x_i is the fraction of a given particle i with a given scattering intensity and D_i is the diameter of the particle i. The polydispersity index (PdI) was calculated from cumulant analysis of the measured dynamic light scattering intensity autocorrelation function. Each sample was measured in triplicate at 25 °C.

2.6.3. Optical microscopy

Emulsions were evaluated at different stages of digestion. Samples were poured onto microscope slides, covered with glass cover slips and observed using a Carl Zeiss Model Axio Scope.A1 optical microscope (Zeiss, Germany). Objective lenses (40 ×) were used to visualize the microstructure of the emulsions.

2.6.4. Free fatty acid release

The amount of free fatty acids (FFA) released from WPI fibril-stabilized emulsion was measured by using a titration method (Pinsirodom & Parkin, 2005) in order to determine the digestion activity. Acetone (10 mL) were added to a collected volume (5 mL) of jejunal filtrate, ileal filtrate and ileal delivery samples to quench the enzymes activity. Afterwards, 3 drops of 1% (w/v) phenolphthalein were added to this mixture as an indicator. A direct titration with 0.1 mol·L^{-1} NaOH using a burette was performed. The percentage of free fatty acids released was calculated as described in eq. (2) from the number of moles of NaOH added until the titration end point divided by the number of moles of FFA that could be produced from triglycerides if they were all digested (assuming 2 FFA produced per 1 triacylglycerol molecule) (Li, Hu, Du, Xiao, & McClements, 2011).

$$\%\text{FFA} = 100 \times \left(\frac{v_{\text{NaOH}} \times m_{\text{NaOH}} \times M_{\text{lipid}}}{w_{\text{lipid}} \times 2} \right) \quad (2)$$

where v_{NaOH} is the volume of sodium hydroxide required to neutralize the FFA generated (in L), m_{NaOH} is the molarity of the sodium hydroxide used (in mol·L^{-1}), w_{lipid} is the total weight of soybean oil initially present and M_{lipid} is the molecular weight of the soybean oil (the molecular weight of soybean oil was considered to be 873 g·mol^{-1} based on their average fatty acid composition).

2.7. Statistical analysis

The experiments were carried out at least in duplicate and the results were reported as averages and standard deviations of these measurements. The results obtained were submitted to variance analysis (ANOVA) and Tukey's test was applied to evaluate significant differences between the mean values ($p < 0.05$).

3. Results

3.1. Morphology and surface charge density of whey protein fibrils

Fibrils produced at the same processing conditions (pH 2, 80 °C/20 h) were evaluated after pH readjustment from 2 to 3 and 7. WPI fibril dispersion showed high positive surface charge density at pH 3 (+ 49 ± 10 mV), resulting from the protonation of the amino groups as the pH is below and far from the isoelectric point WPI (pI ≈ 5). At pH 7 (above the pI), the zeta potential became negative and a lower absolute value was observed (− 33 ± 7 mV). TEM micrographs were taken from WPI nanofibrils at pH 3 and 7 and they are shown in Fig. 2. Linear and long fibrils were observed at pH 3 and the high zeta potential value provided enough electrostatic repulsion, maintaining them dispersed and isolated (Fig. 2A). Increasing the pH value from 3 to 7 led to the formation of shorter and aggregated fibrils as can be seen in Fig. 2. Other authors have reported the reduction of fibril length at pH 7 (Akkermans, Van Der Goot, Venema, Van Der Linden, & Boom, 2008; Jung & Mezzenga, 2010; Kroes-Nijboer et al., 2012; Mantovani et al., 2016b). This result could be attributed to fibril aggregation at the critical pH region near the protein pI that contributes to the collapse of amyloid-type nanostructures as a consequence of pH increase.

3.2. Emulsion stability and microstructure

A concentration of 2% (w/v) WPI was used to prepare emulsions containing 30% (w/w) soybean oil since at these concentrations was possible to produce stable emulsions (Mantovani, Cavallieri, Netto, & Cunha, 2013).

Table 1 shows the energy density input during high-pressure homogenization of O/W emulsions stabilized by WPI fibrils calculated for different homogenization pressures and number of homogenization cycles. The energy density for high-pressure homogenization corresponds to the homogenization pressure multiplied by the number of homogenization cycles (Karbstein & Schubert, 1995). Thus, the energy input during high-pressure homogenization after twenty cycles was 20-fold higher than the energy density for one homogenization cycle at the same homogenization pressure. In this way, the energy density inherent to the homogenization process increased as follows: $P_3C_1 < P_{20}C_1 < P_3C_{20} < P_{20}C_{20}$.

All high-pressure homogenized emulsions showed no signs of phase separation into a top cream phase and a bottom serum phase until 7 days of storage. The particle size distribution (PSD) of emulsions as well as the mean hydrodynamic diameter and polydispersity index (PdI) of each peak are described in Fig. 3. The PdI values range from 0 to 1 (Fig. 3C) in which lower values indicate a more homogeneous PSD. Emulsions at pH 3 showed a monomodal PSD with average hydrodynamic diameter around 770 nm and PdI around 0.3 (Fig. 3A), except for the emulsion produced using the highest energy density ($P_{20}C_{20}$) that presented a shift of the PSD to higher diameters. Such a shift resulted in a bimodal PSD with mean hydrodynamic diameters around 1000 and 200 nm for the peaks 1 and 2, respectively. On the other hand, all emulsions at pH 7 showed bimodal PSD (Fig. 3B) and no significant ($p > 0.05$) differences were observed in the mean hydrodynamic diameters of the first and second peaks for the emulsions at pH 7 and the $P_{20}C_{20}$ emulsion at pH 3. At pH 3, a considerable increase in energy density did not affect significantly the PSD but much higher energy density resulted in larger oil droplet size. For emulsions at pH 7, instead, the increase of energy density led to a decrease in the area of the first peak (larger particles) and a corresponding increase in the area of the second peak (smaller particles). However, a further increase in energy density did not affect the PSD at neutral pH. It has been reported that mechanical treatments promote fracture of fibrils into small segments (Oboroceanu et al., 2011; Oboroceanu et al., 2014; Peng et al., 2016; Serfert et al., 2014). Thus, the appearance of two peaks suggests that the peaks 1 and 2 are related to shortened protein fibrils (pH 3) or small aggregates of fibrils (pH 7) (smaller particles) and oil droplets (larger particles), respectively.

Despite the changes in size distribution (number of peaks), the PSD width was not significantly affected by the pH and energy density and varied from 80 to 2000 nm. On the other hand, the results showed that the average hydrodynamic diameter was highly pH-dependent. In general, the emulsions stabilized by fibrils at pH 3 presented smaller oil droplets than emulsions stabilized by fibrils at neutral pH. Fibrils remain aggregated likely by hydrophobic interactions at neutral pH as can be seen in Fig. 2B. In this way, the increase of the mean droplet size could also be attributed to the higher thickness of the protein layer adsorbed onto the interface (Mantovani et al., 2016a). Moreover, the presence of aggregated fibrils at pH 7 probably hampered oil droplets

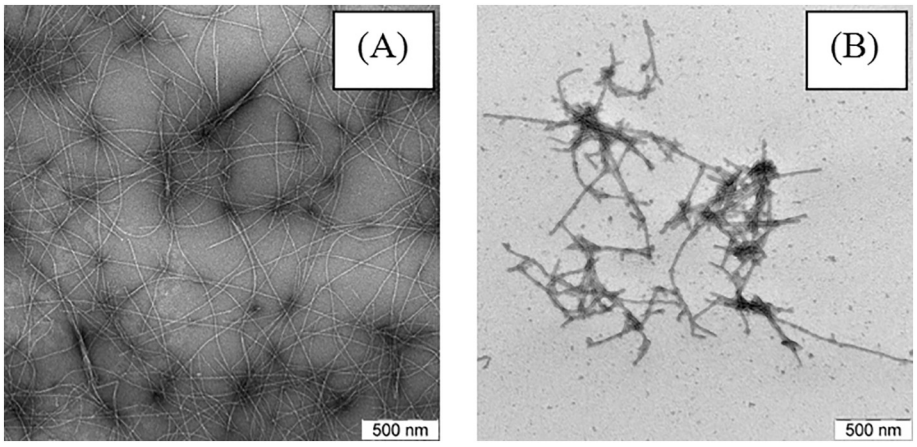

Fig. 2. TEM micrographs of WPI fibrils at (A) pH 3 and (B) pH 7. Scale bar = 500 nm.

Table 1
Energy density input during high-pressure homogenization of emulsions containing 30% (v/v) soybean oil and WPI nanofibrils.

Emulsion	Homogenization pressure (psi)	Number of homogenization cycles	Energy density ($kJ \cdot m^{-3}$)
P_3C_1	3000	1	2.1×10^4
P_3C_{20}		20	4.1×10^5
$P_{20}C_1$	20,000	1	1.4×10^5
$P_{20}C_{20}$		20	2.8×10^6

recovering. The higher amount of energy supplied during high pressure homogenization leads to enhanced collision frequency between the droplets (Jafari et al., 2008), favoring the flocculation or coalescence process. Therefore, an insufficient oil droplets recovering by fibrils could favor a higher droplet size and a further emulsion destabilization during homogenization process or storage (Mantovani et al., 2013).

3.3. *In vitro* digestion

The simulated digestion was performed only with the WPI nanofibrils dispersion and with the emulsion stabilized by fibrils at pH 3 and homogenized at 3000 psi for 1 cycle, since this emulsion showed the smallest oil droplets even when the lowest energy density was applied which is advantageous from the energetic point of view and in terms of emulsion stability. Samples at different stages of the simulated digestion process (before digestion, stomach, duodenum, jejunum and ileum) were evaluated. Simulated oral digestion was not performed since most liquids do not require an oral phase, mainly due to the very short residence times in the oral cavity. Moreover, the simulation of an oral phase in case of liquid food is not important if the meal does not contain starch (Minekus et al., 2014).

3.3.1. *Whey protein nanofibril dispersion*

Initially, *in vitro* digestibility of WPI nanofibril dispersion was evaluated through TEM microscopy (Fig. 4) and native polyacrylamide gel electrophoresis (native-PAGE) (Fig. 5). Before simulated digestion

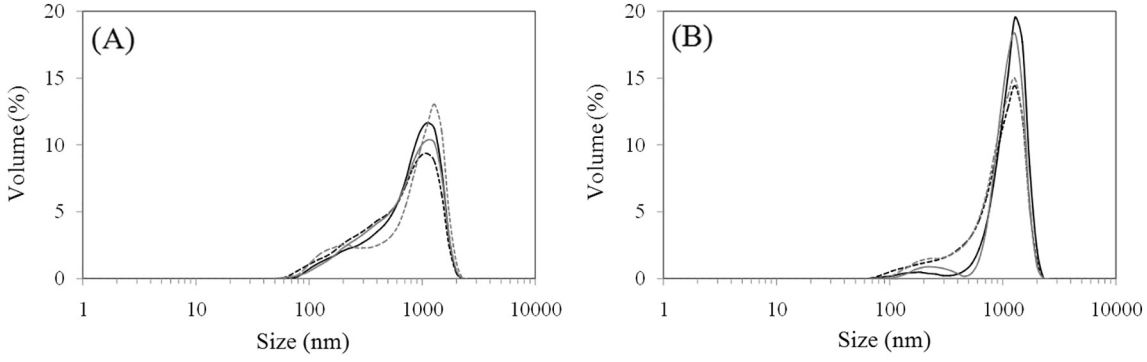

(C)

pH	Emulsion	$\bar{D}$ (nm)		PdI (-)	
		Peak 1	Peak 2	Peak 1	Peak 2
3	P_3C_1	770 ± 36 [a]	-	0.30 ± 0.02 [a]	-
	P_3C_{20}	756 ± 86 [a]	-	0.35 ± 0.04 [a]	-
	$P_{20}C_1$	828 ± 86 [a]	-	0.27 ± 0.03 [a]	-
	$P_{20}C_{20}$	1066 ± 268 [a]	187 ± 58	0.18 ± 0.06 [b]	0.12 ± 0.06
7	P_3C_1	1227 ± 87 [a]	163 ± 38 [a]	0.13 ± 0.05 [ab]	0.09 ± 0.01 [a]
	P_3C_{20}	1107 ± 180 [a]	179 ± 51 [a]	0.17 ± 0.04 [a]	0.09 ± 0.01 [a]
	$P_{20}C_1$	1153 ± 140 [a]	231 ± 53 [a]	0.07 ± 0.03 [b]	0.07 ± 0.02 [a]
	$P_{20}C_{20}$	1299 ± 282 [a]	279 ± 104 [a]	0.10 ± 0.05 [ab]	0.09 ± 0.03 [a]

Fig. 3. Effects of pH, homogenization pressure and number of homogenization cycles on the droplet size distribution of the emulsions containing 30% (v/v) soybean oil and stabilized by WPI fibrils at (A) pH 3 and (B) pH 7. (▬) P_3C_1, (▬ ▬) P_3C_{20}, (▬) $P_{20}C_1$ and (▬ ▬) $P_{20}C_{20}$. (C) Average hydrodynamic diameter ($\bar{D}$) and polydispersity index (PdI) values. Identical letters in the same column for each pH indicate that there are no differences between the measurements ($p > 0.05$).

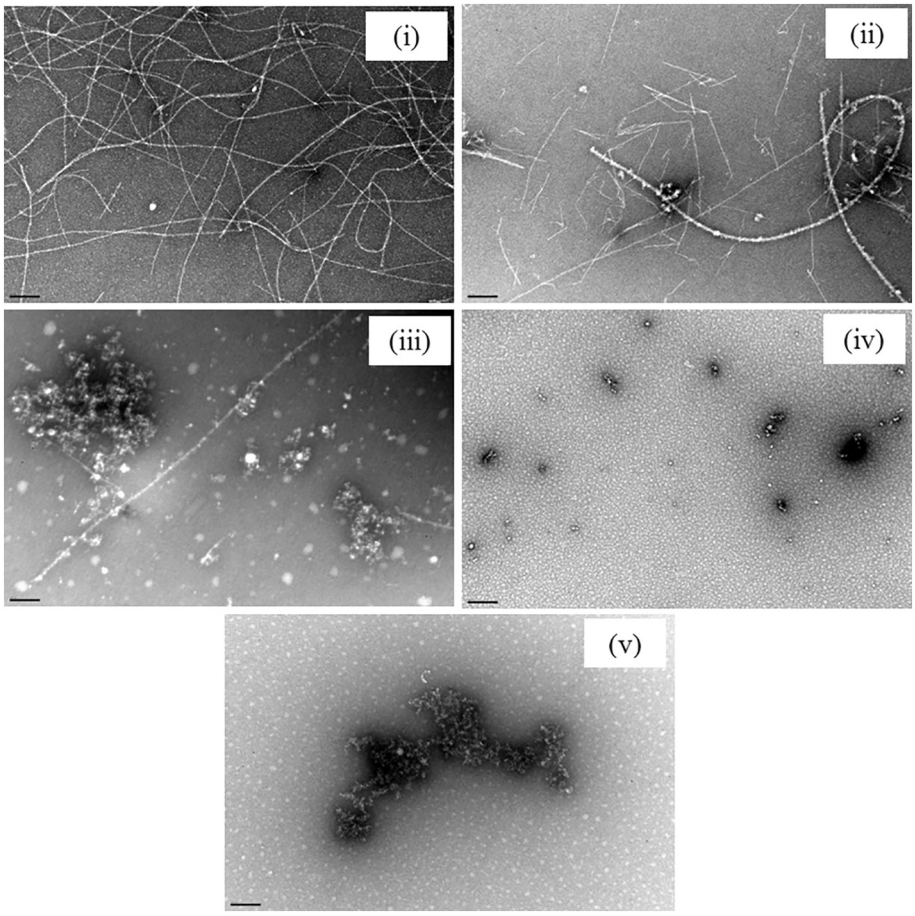

Fig. 4. TEM micrographs of WPI fibrils at various stages of *in vitro* digestion: (i) initial emulsion (before *in vitro* digestion), (ii) stomach, (iii) duodenum, (iv) jejunal filtrate and (v) ileal filtrate. Scale bar = 200 nm.

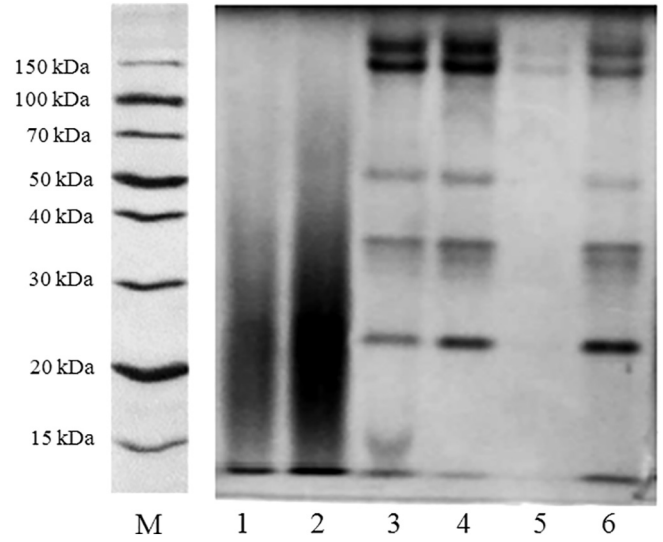

Fig. 5. Native-PAGE electrophoretograms for WPI fibril dispersion at various stages of *in vitro* digestion: (1) initial (before *in vitro* digestion), (2) stomach, (3) duodenum, (4) jejunal filtrate, (5) ileal filtrate and (6) ileal delivery. Lane (M) commercial molecular weight marker.

(Fig. 4i), long and linear fibrils were observed. These characteristics were maintained after the addition of simulated gastric fluid (Fig. 4ii). The presence of WPI amyloid-like structures indicates that these materials have a significant resistance under acidic conditions, high ionic strength and pepsin addition. On the other hand, after simulated intestinal fluids addition (Fig. 4iii–v), large protein aggregates were visualized instead of fibrillar nanostructures. The pH readjustment from 2 (stomach pH) to 7 (intestine pH) may have originated weaker repulsion forces caused by the low surface charge density of fibrils around WPI pI (pH ≈ 5) (Livney, 2010; Mantovani et al., 2016b), thus leading to fibril proximity and favoring hydrophobic interactions and the formation of aggregates that remained even after reaching pH 7.

Fig. 5 shows the native-PAGE profile of initial WPI fibril dispersion in lane 1 which presented a band scattering. A similar electrophoretic profile was observed previously for β-lg nanostructures (Madalena et al., 2016). In lane 2 (Fig. 5), smears remained in the native-PAGE profile after simulated gastric fluid addition. A previous work reported that the electrophoretic profile of the simulated gastric secretion analysed under similar conditions consisted of four bands: two bands around 150 kDa, one band between 30 and 40 kDa and one band between 20 and 30 kDa (Madalena et al., 2016). Thus, the smears observed in lane 2 typical of WPI fibril electrophoretic profile indicate that WPI nanofibrils were resistant to proteolysis and to the severe pH conditions of the simulated gastric digestion. After simulated intestinal fluid addition (lanes 3 to 6), the typical electrophoretic profile of WPI fibrils was not observed. The electrophoretic profiles in lanes 3 to 6 were similar to that ones observed by other authors for the simulated gastric and duodenal secretions (without sample) (Madalena et al., 2016). These results indicate that the initial fibrillar nanostructures disappeared during intestinal digestion (Fig. 5), which is in agreement with TEM results (Fig. 4iii-v). Moreover, much less intense bands were observed in lane 5 in comparison to the bands of electrophoretic profiles of the other simulated intestinal steps. Other studies have reported that the increase of WPI fibril pH from 3 to 7 can result in a loss of amyloid-like structures (Mantovani et al., 2016b; Munialo, Martin, Van der Linden, & de Jongh, 2014). Also, previous findings showed that WPI fibrils presented varied protease resistance depending on the proteolytic enzyme, being more susceptible to pancreatin than to pepsin

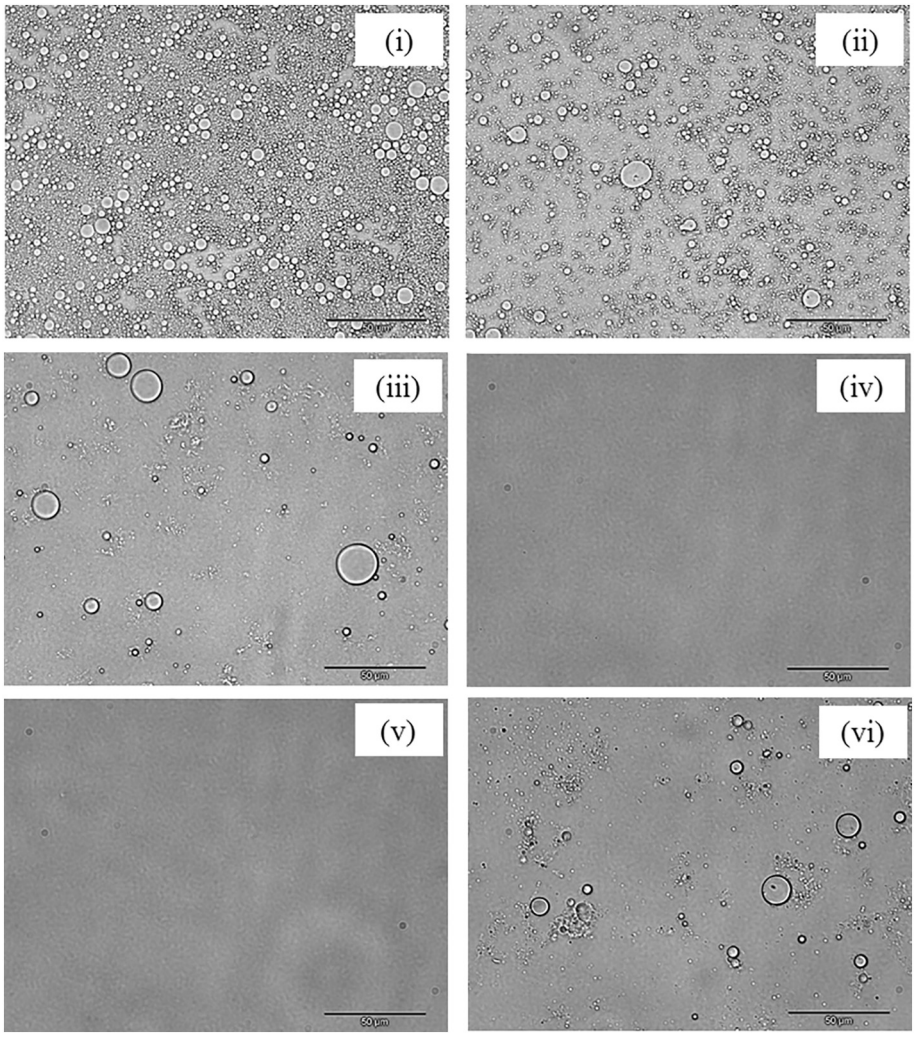

Fig. 6. Optical microscopy and droplet size distribution of emulsion containing 30% (v/v) soybean oil and stabilized by 2% (w/v) WPI fibrils at pH 3 (scale bar = 50 μm) as the emulsion passes through the dynamic *in vitro* digestion model: (i) initial emulsion (before *in vitro* digestion), (ii) stomach, (iii) duodenum, (iv) jejunal filtrate, (v) ileal filtrate and (vi) ileal delivery.

degradation (Lassé et al., 2016). Thus, the changes in electrophoretic profile after simulated intestinal fluid addition indicate that the peptides in fibrils were digested to smaller peptides by pancreatin.

3.3.2. Emulsion stabilized by whey protein nanofibrils

The WPI fibril-stabilized emulsion after the steps of gastric and intestinal *in vitro* digestion was evaluated through optical microscopy (Fig. 6) and droplet size distribution (Fig. 7). The droplet size distribution of the emulsion obtained using dynamic light scattering (DLS) showed that the initial emulsion had a monomodal distribution with a main peak centered around 770 nm. The initial emulsion presented a polydisperse aspect with individual droplets evenly distributed (Fig. 6i) corroborating the relatively high PdI (around 0.3). The addition of simulated gastric fluid resulted in slightly PSD changes as can be seen in Fig. 7A. These minor modifications are associated to a bimodal droplet size distribution, the appearance of a very small second peak in the region of 135 nm (peak 2) and a PSD shift towards bigger hydrodynamic diameters (peak 1). However, the average hydrodynamic diameter of the first peak after gastric fluid addition did not differ significantly ($p > 0.05$) from the average hydrodynamic diameter of the initial emulsion. The increase in droplet size suggests the occurrence of droplet aggregation, coalescence or flocculation due to the action of digestive enzymes as well as changes in pH and ionic strength (Golding et al., 2011; Malaki Nik, Wright, & Corredig, 2010; Mantovani et al., 2013; Pinheiro et al., 2013). The microstructure of the emulsion after simulated gastric fluid addition (Fig. 6ii) showed a polydisperse aspect similar to that observed for the initial emulsion despite some dispersed bigger droplets, confirming the slight changes observed for droplet size distribution (Fig. 7). As previously described, a similar behavior was also observed for fibril dispersion before digestion and after the simulated gastric step. Fibril resistance to simulated gastric digestion (Figs. 4ii and 5) probably kept the O/W interface intact, enhancing the emulsion stability under these adverse environmental conditions.

The addition of simulated intestinal fluids resulted in a bimodal distribution with an increase of the area of the second peak (smaller particles) and a corresponding decrease of the area of the first peak (bigger particles) for the jejunal filtrate. As expected, the duodenal sample and ileal delivery (*i.e.* the fraction that is not absorbed in the small intestine) exhibited higher particle sizes compared to jejunal and ileal filtrates (*i.e.* the fractions absorbed at jejunum and ileum compartments, respectively). In this way, the DLS technique was not suitable for the measurement of particle diameter of the duodenum and ileal delivery sample, since it can measure particle diameters up to few microns (Pinheiro et al., 2013). After addition of simulated intestinal fluids, some big oil droplets could be observed in micrographs of duodenum stage (Fig. 6iii). The emulsion destabilization could be related to the weakening of O/W interface due to fibrillar nanostructures destabilization (Fig. 4iii–v), which favored the displacement of fibrils from the O/W interface by bile salts contained in the simulated intestinal fluids. The oil droplets were not visualized in micrographs of jejunal and ileal filtrates (Fig. 6iv–v). Bile salts facilitate the solubilisation of highly lipophilic digestion products such as FFA into mixed micelles (bile salt/phospholipid micelles) (Small, Cabral, Cistola,

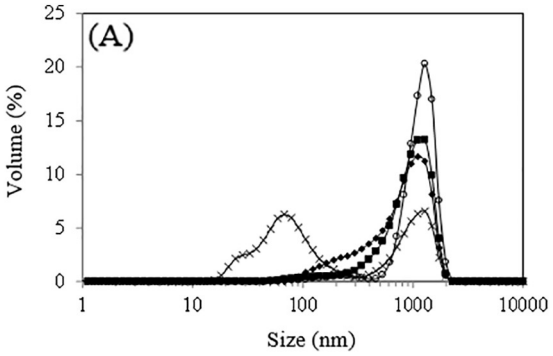

(B)

Digestion step	$\bar{D}$ (nm)		PdI (-)	
	Peak 1	Peak 2	Peak 1	Peak 2
Initial	770 ± 36 ^{c}	-	0.30 ± 0.02 ^{a}	-
Stomach	981 ± 53 ^{bc}	137 ± 13 ^{b}	0.13 ± 0.01 ^{b}	0.076 ± 0.002 ^{c}
Duodenum*	-	-	-	-
Jejunal filtrate	1098 ± 55 ^{abc}	77 ± 41 ^{b}	0.11 ± 0.02 ^{b}	0.28 ± 0.05 ^{a}
Ileal filtrate	1334 ± 157 ^{a}	203 ± 15 ^{a}	0.111 ± 0.002 ^{b}	0.2 ± 0.1 ^{bc}
Ileal delivery*	-	-	-	-

Fig. 7. (A) Droplet size distribution of the emulsion containing 30% (v/v) soybean oil and stabilized by 2% (w/v) WPI fibrils at pH 3 at various stages of *in vitro* digestion: (♦) initial emulsion (before *in vitro* digestion), (■) stomach, (×) jejunal filtrate, (○) ileal filtrate. (B) Average hydrodynamic diameter ($\bar{D}$) and polydispersity index (PdI) values. Identical letters in the same column for each pH indicate that there are no differences between the measurements ($p > 0.05$). *The DLS technique was not suitable for the measurement of particle diameter of these samples.

Parks, & Hamilton, 1984). After the incorporation of lipid digestion products into the mixed micelles, these compounds can be transported to the enterocyte surfaces where they are absorbed from the small intestine into the bloodstream (McClements & Xiao, 2012). Thus, the duodenal sample probably consisted of protein aggregates (Fig. 4iv–v) and mixed micelles that were supposed to cross the simulated intestinal barrier, besides big oil droplets. This result would explain the appearance of a second peak of hydrodynamic diameter around 200 nm in the jejunal filtrate (Fig. 7) as well as the absence of oil droplets in the micrograph (Fig. 6iv). On the other hand, big droplets can be seen in ileal delivery, suggesting that remaining droplets would be eliminated by the gastrointestinal tract according to this simulated *in vitro* digestion. Bile salts present a low hydrophilic-lipophilic balance (HLB) number, being ineffective in stabilizing oil-in-water emulsions against coalescence (Mun et al., 2007).

3.3.2.1. Free fatty acid release. The rate of fat digestibility is controlled by surface accessibility, which is determined by surfactant chemistry and mainly by the emulsion interfacial area (Golding et al., 2011). A measure of fat digestibility is the production of free fatty acids (FFA). It allows determining the capability of these systems to protect the emulsified lipid against lipolysis. Fig. 8 shows the results for the production of FFA during the simulated intestinal digestion of WPI fibril-stabilized emulsions. The emulsions showed an increased amount of FFA production throughout the simulated intestinal digestion. This result indicates that the interfacial weakening could be attributed to binding of bile salts. The displacement of fibrils by bile salts favored the binding of lipase, enabling lipolysis (Hur, Decker, & McClements, 2009). The percentage of FFA adsorbed in the simulated small intestine (jejunum and ileum) conditions (43 ± 7%) is much lower than the total percentage of FFA released (102 ± 6%). Moreover, it was not observed significant difference between cumulative percentages of FFA release in jejunal filtrate and ileal filtrate (Fig. 8). Thus, FFA absorption occurred mostly in simulated jejunal step. This is in accordance with the electrophoretic results (Fig. 5) that showed much less intense bands in ileal filtrate (lane 5) than bands in jejunal filtrate (lane 4) and ileal delivery (lane 6). Nowadays, there is a great concern that excessive consumption of fat-rich products is resulting in increased chronic human disease occurrence (*e.g.*, obesity, coronary heart disease, and diabetes). Consequently, trying to develop reduced fat products with acceptable physicochemical and sensory properties is often challenging because of the multiple roles that fat droplets play in determining the overall quality of food products (*e.g.*, optical properties, texture, flavor profile and satiety) (Chung, Smith, Degner, & McClements, 2016; McClements, 2005). Multilayer coatings can be designed to reduce the caloric content of foods by preventing lipases from accessing encapsulated lipids (McClements, 2010). Other authors have reported that nanoemulsions stabilized by lactoferrin (primary emulsion) presented a high percentage of FFA absorbed in simulated intestinal conditions (64 ± 6%) (Pinheiro et al., 2016). This value was reduced to 54 ± 11% by the addition of an alginate coating (secondary emulsion). Only after the addition of a second biopolymer layer, the FFA absorbed result was similar to that one obtained for WPI fibril-stabilized emulsion. Thus, the WPI fibril-stabilized emulsion has significant potential for being applied as a primary emulsion to develop a multilayer emulsion aiming at reducing the absorption of FFA.

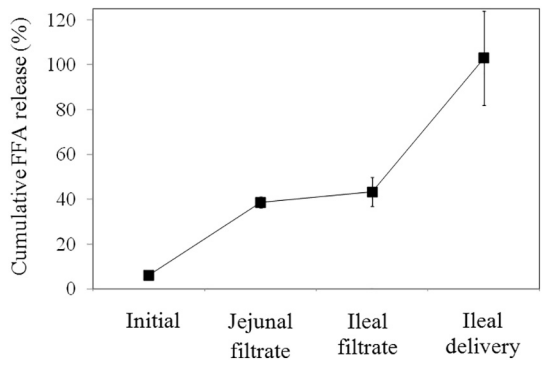

Fig. 8. Percentage of free fatty acids (FFA) released from emulsion containing 30% (v/v) soybean oil and stabilized by 2% (w/v) WPI fibrils at pH 3 as it passes through the dynamic *in vitro* digestion model.

4. Conclusion

High-pressure homogenized emulsions containing WPI fibrils were stable during one week. The droplet size distribution of the emulsions was pH-dependent and smaller droplet sizes (in the order of 770 nm) were obtained at acidic pH independent of the energy density of the homogenization process. Concerning the *in vitro* digestion response using a dynamic digestion model, the WPI fibrils-stabilized emulsion was stable under simulated gastric conditions but destabilized in the simulated intestinal conditions. The physicochemical stability of the

WPI fibril dispersion within the simulated gastrointestinal tract was similar to that observed for the emulsion. This fact confirms the significant impact of the interface characteristics on the emulsion digestion. Although a high amount of FFA was released, the use of WPI fibrils as emulsifier resulted in reduced absorption of FFA in the simulated intestinal conditions and, consequently, in reduced calorie absorption without reducing calorie intake. Further works aiming at comparing the response of emulsions stabilized by whey protein fibrils with emulsions stabilized by native whey proteins under the same simulated gastrointestinal conditions or applying whey protein fibrils in more complex systems would be interesting.

Supplementary data to this article can be found online at http://dx.doi.org/10.1016/j.foodres.2017.06.049.

Acknowledgements

The authors would like to thank Coordenação de Aperfeiçoamento de Pessoal de Nível Superior (CAPES) for the PhD fellowship and the financial support (CAPES/FCT n° 7362/14-5 and CAPES/FCT nº 349/13). The author Ana C. Pinheiro is recipient of a fellowship from the Fundação para a Ciência Tecnologia (FCT, Portugal) through grant SFRH/BPD/101181/2014. We acknowledge INCT/INOMAT for supporting TEM analysis of fibril characterization carried out by Douglas Soares da Silva. We also would like to acknowledge Daniel A. Madalena for the contribution with the representative schematic of the *in vitro* dynamic digestion system.

References

Akkermans, C., Van Der Goot, A. J., Venema, P., Van Der Linden, E., & Boom, R. M. (2008). Properties of protein fibrils in whey protein isolate solutions: Microstructure, flow behaviour and gelation. *International Dairy Journal*, *18*, 1034–1042.

Bateman, L., Ye, A., & Singh, H. (2010). In vitro digestion of beta-lactoglobulin fibrils formed by heat treatment at low pH. *Journal of Agricultural and Food Chemistry*, *58*, 9800–9808.

Blijdenstein, T. B. J., Veerman, C., & Van der Linden, E. (2004). Depletion-flocculation in oil-in-water emulsions using fibrillar protein assemblies. *Langmuir*, *20*, 4881–4884.

Chung, C., Smith, G., Degner, B., & McClements, D. J. (2016). Reduced fat food emulsions: Physicochemical, sensory, and biological aspects. *Critical Reviews in Food Science and Nutrition*, *56*, 650–685.

Golding, M., Wooster, T. J., Day, L., Xu, M., Lundin, L., Keogh, J., & Clifton, P. (2011). Impact of gastric structuring on the lipolysis of emulsified lipids. *Soft Matter*, *7*, 3513–3523.

Guzey, D., & McClements, D. J. (2006). Formation, stability and properties of multilayer emulsions for application in the food industry. *Advances in Colloid and Interface Science*, *128*, 227–248.

Hu, M., McClements, D. J., & Decker, E. A. (2003). Lipid oxidation in corn oil-in-water emulsions stabilized by casein, whey protein isolate, and soy protein isolate. *Journal of Agricultural and Food Chemistry*, *51*, 1696–1700.

Hur, S. J., Decker, E. A., & McClements, D. J. (2009). Influence of initial emulsifier type on microstructural changes occurring in emulsified lipids during in vitro digestion. *Food Chemistry*, *114*, 253–262.

Jafari, S. M., Assadpoor, E., He, Y., & Bhandari, B. (2008). Re-coalescence of emulsion droplets during high-energy emulsification. *Food Hydrocolloids*, *22*, 1191–1202.

Jung, J.-M., & Mezzenga, R. (2010). Liquid crystalline phase behavior of protein fibers in water: Experiments versus theory. *Langmuir*, *26*, 504–514.

Karbstein, H., & Schubert, H. (1995). Developments in the continuous mechanical production of oil-in-water macro-emulsions. *Chemical Engineering and Processing: Process Intensification*, *34*, 205–211.

Kroes-Nijboer, A., Sawalha, H., Venema, P., Bot, A., Floeter, E., Den Adel, R., ... Van der Linden, E. (2012). Stability of aqueous food grade fibrillar systems against pH change. *Faraday Discussions*, *158*, 125–138.

Laemmli, U. K. (1970). Cleavage of structural proteins during the assembly of the head of bacteriophage T4. *Nature*, *227*(5259), 680–685.

Lassé, M., Ulluwishewa, D., Healy, J., Thompson, D., Miller, A., Roy, N., ... Gerrard, J. A. (2016). Evaluation of protease resistance and toxicity of amyloid-like food fibrils from whey, soy, kidney bean, and egg white. *Food Chemistry*, *192*, 491–498.

Li, Y., Hu, M., Du, Y., Xiao, H., & McClements, D. J. (2011). Control of lipase digestibility of emulsified lipids by encapsulation within calcium alginate beads. *Food Hydrocolloids*, *25*, 122–130.

Livney, Y. D. (2010). Milk proteins as vehicles for bioactives. *Current Opinion in Colloid & Interface Science*, *15*, 73–83.

Loveday, S. M., Rao, M. A., Creamer, L. K., & Singh, H. (2009). Factors affecting rheological characteristics of fibril gels: The case of beta-lactoglobulin and alpha-lactalbumin. *Journal of Food Science*, *74*, R47–R55.

Loveday, S. M., Su, J., Rao, M. A., Anema, S. G., & Singh, H. (2011). Effect of calcium on the morphology and functionality of whey protein nanofibrils. *Biomacromolecules*, *12*, 3780–3788.

Madalena, D. A., Ramos, Ó. L., Pereira, R. N., Bourbon, A. I., Pinheiro, A. C., Malcata, F. X., ... Vicente, A. A. (2016). In vitro digestion and stability assessment of β-lactoglobulin/riboflavin nanostructures. *Food Hydrocolloids*, *58*, 89–97.

Malaki Nik, A., Wright, A. J., & Corredig, M. (2010). Surface adsorption alters the susceptibility of whey proteins to pepsin-digestion. *Journal of Colloid and Interface Science*, *344*, 372–381.

Mantovani, R. A., Cavallieri, Â. L. F., & Cunha, R. L. (2016a). Gelation of oil-in-water emulsions stabilized by whey protein. *Journal of Food Engineering*, *175*, 108–116.

Mantovani, R. A., Cavallieri, A. L. F., Netto, F. M., & Cunha, R. L. (2013). Stability and in vitro digestibility of emulsions containing lecithin and whey proteins. *Food & Function*, *4*, 1322–1331.

Mantovani, R. A., Fattori, J., Michelon, M., & Cunha, R. L. (2016b). Formation and pH-stability of whey protein fibrils in the presence of lecithin. *Food Hydrocolloids*, *60*, 288–298.

McClements, D. J. (2005). *Food emulsions: Principles, practices, and techniques*. CRC Press.

McClements, D. J. (2010). Design of nano-laminated coatings to control bioavailability of lipophilic food components. *Journal of Food Science*, *75*, R30–R42.

McClements, D. J., Decker, E. A., & Park, Y. (2007). *18 - Physicochemical and structural aspects of lipid digestion. Understanding and controlling the microstructure of complex foods*. Woodhead Publishing.

McClements, D. J., & Xiao, H. (2012). Potential biological fate of ingested nanoemulsions: Influence of particle characteristics. *Food & Function*, *3*, 202–220.

Minekus, M., Alminger, M., Alvito, P., Ballance, S., Bohn, T., Bourlieu, C., ... Brodkorb, A. (2014). A standardised static in vitro digestion method suitable for food – An international consensus. *Food & Function*, *5*, 1113.

Mun, S., Decker, E. A., & McClements, D. J. (2007). Influence of emulsifier type on in vitro digestibility of lipid droplets by pancreatic lipase. *Food Research International*, *40*, 770–781.

Munialo, C. D., Martin, A. H., Van der Linden, E., & de Jongh, H. H. J. (2014). Fibril formation from pea protein and subsequent gel formation. *Journal of Agricultural and Food Chemistry*, *62*, 2418–2427.

Oboroceanu, D., Wang, L., Kroes-Nijboer, A., Brodkorb, A., Venema, P., Magner, E., & Auty, M. A. E. (2011). The effect of high pressure microfluidization on the structure and length distribution of whey protein fibrils. *International Dairy Journal*, *21*, 823–830.

Oboroceanu, D., Wang, L., Magner, E., & Auty, M. A. E. (2014). Fibrillization of whey proteins improves foaming capacity and foam stability at low protein concentrations. *Journal of Food Engineering*, *121*, 102–111.

Pafumi, Y., Lairon, D., De la Porte, P. L., Juhel, C., Storch, J., Hamosh, M., & Armand, M. (2002). Mechanisms of inhibition of triacylglycerol hydrolysis by human gastric lipase. *Journal of Biological Chemistry*, *277*, 28070–28079.

Peng, J., Simon, J. R., Venema, P., & Van der Linden, E. (2016). Protein fibrils induce emulsion stabilization. *Langmuir*, *32*, 2164–2174.

Pinheiro, A. C., Coimbra, M. A., & Vicente, A. A. (2016). In vitro behaviour of curcumin nanoemulsions stabilized by biopolymer emulsifiers – Effect of interfacial composition. *Food Hydrocolloids*, *52*, 460–467.

Pinheiro, A. C., Lad, M., Silva, H. D., Coimbra, M. A., Boland, M., & Vicente, A. A. (2013). Unravelling the behaviour of curcumin nanoemulsions during in vitro digestion: Effect of the surface charge. *Soft Matter*, *9*, 3147–3154.

Pinsirodom, P., & Parkin, K. L. (2005). In R. E. Wrolstad (Ed.), *Lipase assays. Handbook of food analytical chemistry* (pp. 371–383). Hoboken, NJ: Wiley.

Pugnaloni, L. A., Dickinson, E., Ettelaie, R., Mackie, A. R., & Wilde, P. J. (2004). Competitive adsorption of proteins and low-molecular-weight surfactants: Computer simulation and microscopic imaging. *Advances in Colloid and Interface Science*, *107*, 27–49.

Serfert, Y., Lamprecht, C., Tan, C. P., Keppler, J. K., Appel, E., Rossier-Miranda, F. J., ... Schwarz, K. (2014). Characterisation and use of β-lactoglobulin fibrils for microencapsulation of lipophilic ingredients and oxidative stability thereof. *Journal of Food Engineering*, *143*, 53–61.

Small, D. M., Cabral, D. J., Cistola, D. P., Parks, J. S., & Hamilton, J. A. (1984). The ionization behavior of fatty acids and bile acids in micelles and membranes. *Hepatology*, *4*, 77S–79S.

Torcello-Gomez, A., Maldonado-Valderrama, J., Martin-Rodriguez, A., & McClements, D. J. (2011). Physicochemical properties and digestibility of emulsified lipids in simulated intestinal fluids: Influence of interfacial characteristics. *Soft Matter*, *7*, 6167–6177.

Walstra, P. (2003). *Physical chemistry of foods*. New York: Marcel Dekker.